Ann. Geophys., 25, 2019–2027, 2007
www.ann-geophys.net/25/2019/2007/

Annales Geophysicae

Variations of topside ionospheric scale heights over Millstone Hill during the 30-day incoherent scatter radar experiment

L. Liu[1], W. Wan[1], M.-L. Zhang[1], B. Ning[1], S.-R. Zhang[2], and J. M. Holt[2]

[1]Institute of Geology and Geophysics, Chinese Academy of Sciences, Beijing 100029, China
[2]Haystack Observatory, Massachusetts Institute of Technology, Westford, MA, USA

Received: 22 May 2007 – Revised: 11 August 2007 – Accepted: 18 September 2007 – Published: 2 October 2007

Abstract. A 30-day incoherent scatter radar (ISR) experiment was conducted at Millstone Hill (288.5° E, 42.6° N) from 4 October to 4 November 2002. The altitude profiles of electron density N_e, ion and electron temperature (T_i and T_e), and line-of-sight velocity during this experiment were processed to deduce the topside plasma scale height H_p, vertical scale height VSH, Chapman scale height H_m, ion velocity, and the relative altitude gradient of plasma temperature (dT_p/dh)/T_p, as well as the F_2 layer electron density (N_mF$_2$) and height (h_mF$_2$). These data are analyzed to explore the variations of the ionosphere over Millstone Hill under geomagnetically quiet and disturbed conditions. Results show that ionospheric parameters generally follow their median behavior under geomagnetically quiet conditions, while the main feature of the scale heights, as well as other parameters, deviated significantly from their median behaviors under disturbed conditions. The enhanced variability of ionospheric scale heights during the storm-times suggests that the geomagnetic activity has a major impact on the behavior of ionospheric scale heights, as well as the shape of the topside electron density profiles. Over Millstone Hill, the diurnal behaviors of the median VSH and H_m are very similar to each other and are not so tightly correlated with that of the plasma scale height H_p or the plasma temperature. The present study confirms the sensitivity of the ionospheric scale heights over Millstone Hill to thermal structure and dynamics. The values of VSH/H_p tend to decrease as (dT_p/dh)/T_p becomes larger or the dynamic processes become enhanced.

Keywords. Ionosphere (Ionospheric disturbances; Mid-latitude ionosphere; Plasma temperature and density)

1 Introduction

The ionospheric scale height, as a measure of the shape of electron density (N_e) profiles or the altitude dependence of electron density, is one of the key ionospheric parameters, due to its intrinsic connection to the ionospheric dynamics, plasma temperature and compositions (Luan et al., 2006; Stankov and Jakowski, 2006b). Several definitions of the ionospheric scale heights exist (Liu et al., 2007). In order to facilitate a description, we adopt the following definitions of ionospheric scale heights. The plasma scale height (H_p) is defined as $k_b(T_i+T_e)/m_i g$, where k_b is the Boltzmann constant, g the acceleration due to gravity, m_i the ion mass, and T_i and T_e the ion and electron temperatures. The

Correspondence to: L. Liu
(liul@mail.iggcas.ac.cn)

ionosondes. The diurnal and seasonal variations of H_m over Hainan (109.0° E, 19.4° N) have been reported by Zhang et al. (2006). Furthermore, the seasonal and solar activity features of H_m over Millstone Hill (288.5° E, 42.6° N) have been investigated with ISR observations (Lei et al., 2005) and over Wuhan (114.4° E, 30.6° N) with digisonde measurements (Liu et al., 2006). They found that H_m over Millstone Hill is overestimated by the IRI2001 model (Bilitza, 2001) and the temporal variations of H_m can be explained in terms of those in the slab thickness. Liu et al. (2006) reported that a moderate positive correlation is found between H_m and the F_2 layer peak height (h_mF_2) and a strong correlation between the bottomside thickness parameter B_0 and H_m. A common feature is found at 13 global stations; that is, the values of H_m are highest in summer and lowest in winter during daytime. It is interesting that, however, the annual variation of H_m becomes much weaker or disappears from late night to pre-sunrise. Recently, Liu et al. (2007) conducted a statistical analysis on the diurnal, seasonal, and solar cycle variations of ionospheric scale heights from the 1966–2002 ISR measurements at Arecibo (293.2° E, 18.3° N; geomagnetic latitude 30°), Puerto Rico. Their statistical analysis identified a clear solar activity pattern of VSH, H_m, and H_p over Arecibo. Median values of H_m over Arecibo are also found to be highest in summer and lowest in winter during daytime, while it exhibits a much weaker seasonal variation at night. They discussed the similarities/differences and quantitative relationships between these ionospheric scale heights over Arecibo and found that the diurnal behaviors of VSH and H_m are much more complicated than that of H_p.

However, the knowledge of the behavior of the ionospheric scale heights remains insufficient. For example, few works study the storm-time variations of the ionospheric scale heights so far. Fortunately, available accumulated databases of ISR (e.g. Zhang et al., 2004, 2005; Tepley, 1997; Isham et al., 2000), topside sounders (Bilitza et al., 2006) and radio occultation measurements, are extremely valuable data sources for investigating the characteristics of the ionospheric scale heights.

An extended ISR campaign was conducted at Millstone Hill from 4 October to 4 November 2002. This experiment covered both geomagnetically quiet and active periods, providing a unique opportunity to explore the variations of the ionosphere. Combining with the simultaneous observation of EISCAT Svalbard Radar, Zhang et al. (2005) studied the ionospheric variability and found that quasi-periodic oscillations (with periods longer than 1 day) were correlated with neutral composition changes originating from geomagnetic activity. Later, Lei et al. (2006) compared those measurements with the prediction of the IRI2001 model. It is found that IRI2001 is in good agreement with the observed h_mF_2 and foF_2 while it overestimates the topside N_e profiles over Millstone Hill.

In this paper, we deduce ionospheric scale heights (H_p, VSH and H_m), the F_2 layer peak electron density (N_mF_2) and height (h_mF_2), ion velocity, and the altitude gradient of plasma temperature from this ISR observation. The first objective of this analysis is to explore the variations of the ionosphere over Millstone Hill under geomagnetically quiet and disturbed conditions. We will focus on the median behavior of the topside scale heights and their behaviors under geomagnetically quiet and disturbed conditions. Another objective is to investigate the correlations between VSH/Hp and the thermal structure and diffusion processes in the ionosphere over Millstone Hill.

2 Data source and solar-geophysical conditions

An ISR experiment was carried out at Millstone Hill from 4 October to 4 November 2002 (Lei et al., 2006; Zhang et al., 2005). The altitudinal profiles of electron density, N_e, ion and electron temperatures, T_i and T_e, and line-of-sight velocity, V_o, were provided from the single-pulses and alternating code measurements. V_o is essentially the vertical ion velocity V_{iz} during this measurement because the zenith angle of radar beams used is close to the vertical direction (88°). In this study, the single-pulses mode data during this experiment are used for investigation.

Figure 1 illustrates the solar-geophysical conditions during this ISR experiment. The 10.7 cm solar radio flux F_{107}, a standard solar activity proxy, takes values between 155.1 to 182.5 units ($10^{-22}\,W\,m^{-2}\,Hz^{-1}$) during the period from 4 October to 4 November 2002 (day numbers 277–308), while its 81-day average F_{107A} is about 174 units. Magnetic indices AE, A_p, and D_{st} are also plotted in Fig. 1. As can be seen from Fig. 1, three geomagnetic disturbances occurred during this period that caused severe ionospheric effects (Zhang et al., 2005).

When considering the geomagnetic activity effects, a reference level should be selected. There are usually two kinds of reference levels used for the purpose: values from quiet day(s) (21 October for this period), or median values from an extended period (say, 30 days). The median values during this interval served as the reference level for this study.

3 Analysis and results

3.1 Analysis method

More than 10 000 altitudinal profiles of N_e, T_e, T_i, and V_o were provided from this Millstone Hill ISR experiment. Figure 2 is an example showing the data processing and analysis procedure we adopted. First, median N_e profiles are evaluated from raw N_e profiles within every 30-min interval in each day. Then N_mF_2 and h_mF_2 are obtained with a least-squares fitting for the median profiles with a Chapman-α function (e.g. Rishbeth and Garriott, 1969),

$$N_e(h) = N_mF_2 \exp\left\{0.5\left[1-z-\exp(-z)\right]\right\},$$

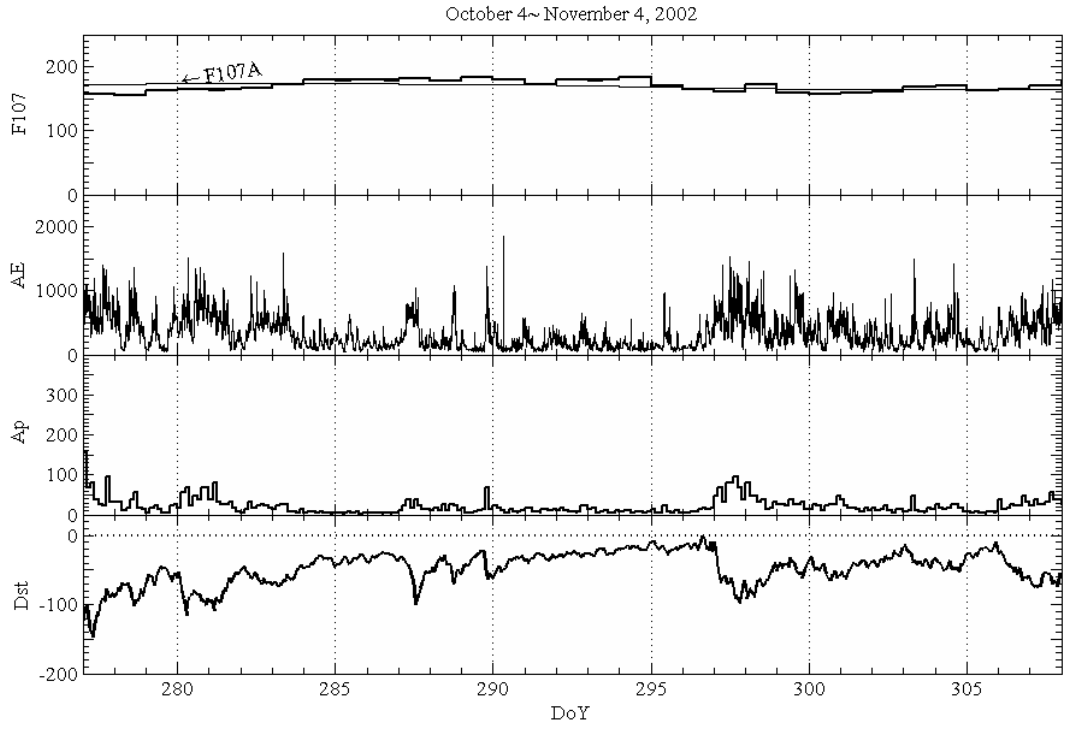

Fig. 1. The solar geophysical conditions during the long-duration Millstone Hill ISR experiment from 4 October and 4 November 2002.

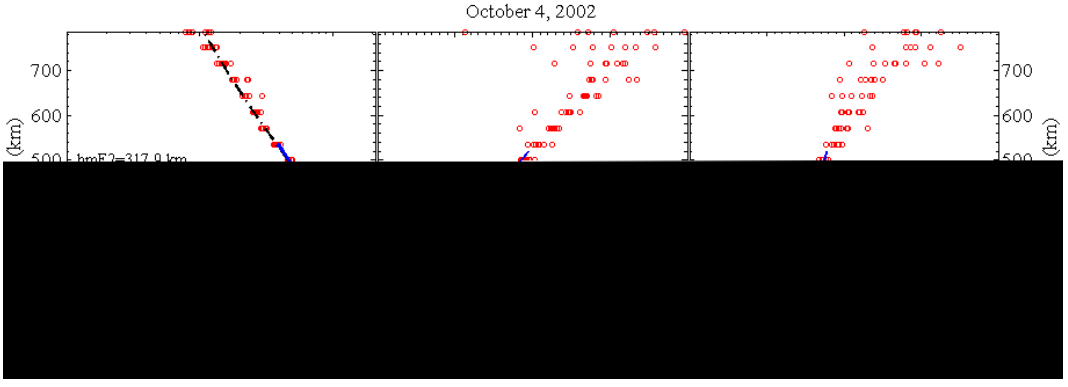

Fig. 2. The Millstone Hill ISR altitude profiles of electron density, N_e, and ion and electron temperatures, T_i and T_e, during a half-hour interval around 17:50 UT on 4 October 2002. At the left panel, the dashed line shows the fit of N_e with a Chapman-α profile function, while the solid line shows the exponential fit. The solid lines at the center and right panels show, respectively, the linear fit for the T_i and T_e profiles.

$$z = (h - h_m\mathrm{F}_2)\big/H(h). \quad (1)$$

Here the Chapman scale height $H(h)$ is assumed to be of linear dependence on altitude (see Lei et al., 2006; Liu et al., 2007). We denote $H(h)$ at $h_m\mathrm{F}_2$ as H_m in Eq. (1). $N_m\mathrm{F}_2$, $h_m\mathrm{F}_2$ and H_m are adjustable variables in the least-squares fitting for median profiles, according to Eq. (1).

An example is shown in the left panel of Fig. 2, in which circle points denote the observed N_e within a half-hour interval centered at 17:50 UT on 4 October 2002, whereas the dashed curve stands for the fitted result with a Chapman function.

We fit each median N_e profile with a Chapman-α function, thus $N_m\mathrm{F}_2$, $h_m\mathrm{F}_2$ and H_m are determined with the least-squares fitting procedure. Good fitting prevails in most cases, and we discard those profiles when significant deviations occur, although those profiles may represent the actual situations. Then the values of vertical scale height, VSH, are obtained from the ($h_m\mathrm{F}_2$+25 km to $h_m\mathrm{F}_2$+250 km) altitude interval of median ISR N_e profiles through a linear fitting for

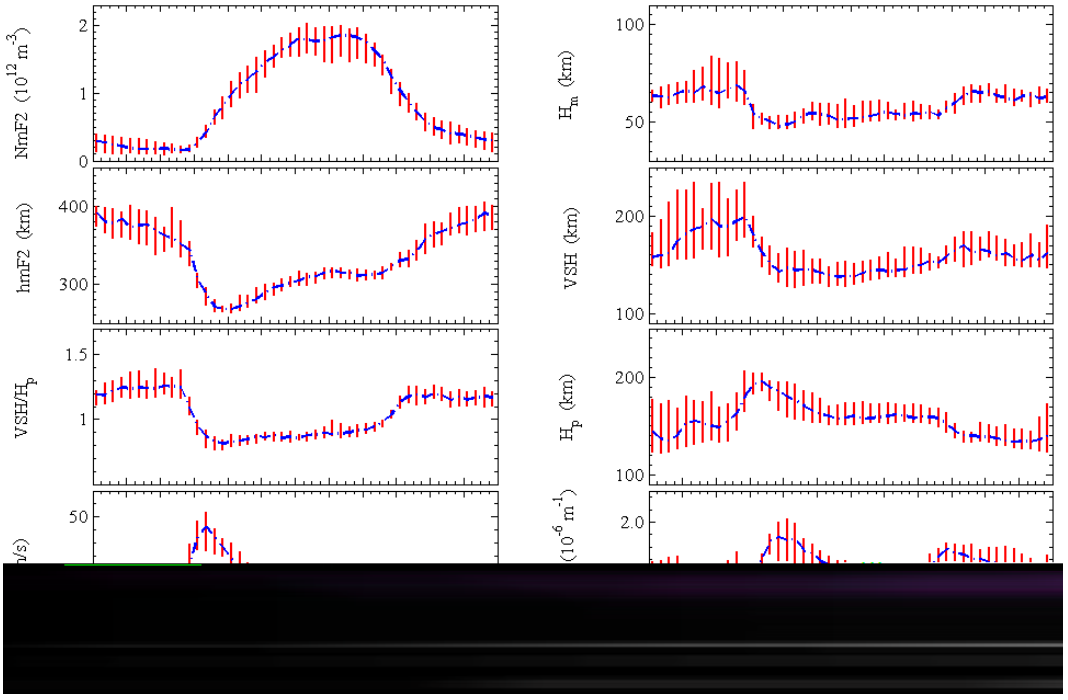

Fig. 3. The diurnal variation of $N_m\mathrm{F}_2$, $h_m\mathrm{F}_2$, the line-of-sight velocity V_o (around 500 km), the Chapman scale height H_m, the vertical scale height VSH, plasma scale height H_p, and the relative gradient of plasma temperatures (dT_p/dh)/T_p derived from the ISR experiment at Millstone Hill. The ratio of VSH to H_p is also plotted. Lines with bars represent, respectively, the half-hourly median values and the corresponding upper (UQ) and lower (LQ) quartiles during the ISR experiment.

ln(N_e) versus h. At the same time, ion and electron temperatures (T_i and T_e) and their altitude gradients (dT_i/dh and dT_e/dh) at an altitude of 100 km above the F_2 peak are also evaluated from a linear fitting ($h_m\mathrm{F}_2$ to $h_m\mathrm{F}_2$+200 km) for the observed T_i and T_e profiles, as shown in the center and right panels of Fig. 2. Thus, H_p and the relative altitude gradient of plasma temperature, (dT_p/dh)/T_p, can be easily determined from the fitted T_i and T_e and their gradients (dT_i/dh and dT_e/dh). T_p is the plasma temperature. Finally, a half-hourly average of ion velocity V_o at an altitude of around 500 km is determined from the raw ISR line-of-sight velocity observations.

3.2 The median pattern of ionospheric parameters

A statistically average feature of the ionosphere can be de-

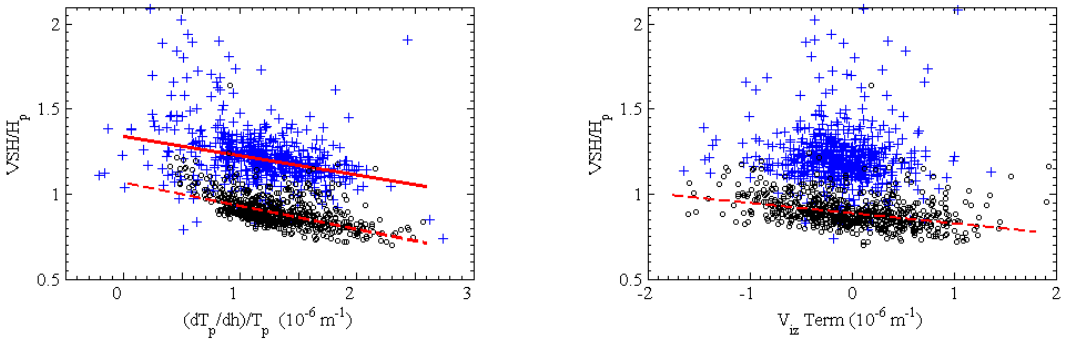

Fig. 4. (Left) Scatterplots of the relative gradient of plasma temperature $(dT_p/dh)/T_p$ versus VSH/Hp, the ratio of the vertical scale height VSH to plasma scale height H_p. (Right) Scatterplots of the velocity term in Eq. (2) versus VSH/H_p. The curves show the fitting linear trends. In each panel, symbol "+" denotes nighttime values while symbol "o" for daytime values.

to a later time in H_p. Moreover, there are also peaks in V_o and $(dT_p/dh)/T_p$ over Millstone Hill when the morning peak is present in H_p. A second peak is quite significant in $(dT_p/dh)/T_p$ at Millstone Hill, according to Fig. 3. One interesting point is that the nighttime values of $(dT_p/dh)/T_p$ at Millstone Hill are quite larger than those at Arecibo (Liu et al., 2007).

3.3 The correlation of VSH/H_p versus $(dT_p/dh)/T_p$ and V_{iz}

By considering the vertical drift and ignoring the horizontal gradient in the ionosphere, Liu et al. (2007) derived a relationship between VSH, H_p, $(dT_p/dh)/T_p$, and the vertical diffusion velocity of ions, W_D, as

$$\frac{1}{\mathrm{VSH}} = \frac{1}{H_p} + \frac{m_i \nu_{in} W_D}{k_b T_p} + \frac{1}{T_p}\frac{dT_p}{dh}. \quad (2)$$

Here k_b is the Boltzmann constant, m_i the ion mass, and ν_{in} is the collision frequency of ions with neutrals.

Equation (1) suggests that the relationship between VSH and H_p is sensitive to the thermal structure and dynamics in the ionosphere. According to Eq. (1), as has been mentioned by Liu et al. (2007), VSH is equal to H_p, if the topside ionosphere is in a state dominated by diffusive equilibrium (W_D=0) and the altitude gradient of the thermal structure can be ignored. However, results at both Arecibo and Millstone Hill illustrate that the altitude gradients of plasma temperatures (dT_p/dh) are significant in the topside temperature profiles during some local time intervals. Furthermore, besides the contributions from the topside temperature structure, the diffusion process ($W_D \neq 0$) can also greatly influence the shape of the topside profiles over Arecibo and Millstone Hill (Luan et al., 2006). Thus, as shown in Fig. 3, VSH will generally deviate from H_p. As a result, VSH might not be so tightly correlated with the plasma temperature or H_p, as originally expected.

Utilizing this ISR measurement, we can investigate the relationships between VSH/H_p and $(dT_p/dh)/T_p$ and the vertical velocity of ions over Millstone Hill, as predicted by Eq. (1). The left panel of Fig. 4 shows the correlation between VSH/H_p and $(dT_p/dh)/T_p$ over Millstone Hill during this experiment. The symbol "+" denotes nighttime values while symbol "o" is used for daytime values. According to the left panel of Fig. 4, the observed tendency of VSH/H_p versus $(dT_p/dh)/T_p$ over Millstone Hill during this experiment supports the prediction of Eq. (1); that is, during both the daytime and nighttime, values of VSH/H_p tend to decrease as $(dT_p/dh)/T_p$ becomes larger. This feature is also found at Arecibo, as reported by Liu et al. (2007). Therefore, we can infer that the topside thermal structure can strongly influence the shape of the topside ionosphere. Further investigation reveals that the contribution of $(dT_p/dh)/T_p$ is mainly to VSH but not to H_p (figure not shown here).

We can also investigate the quantitative relationships between VSH/H_p and the vertical velocity of ions over Millstone Hill. Unfortunately, there is no observed information on neutral wind and the electric field during this measurement. Thus, we cannot deduce diffusion velocity from the line-of-sight velocity V_o for this experiment. To avoid introducing artificial information, we directly use V_{iz} as an approximation to W_D. The right panel of Fig. 4 illustrates the correlation between VSH/H_p and the term related to the vertical velocity of ions in Eq. (1). Symbol "+" again denotes nighttime values while symbol "o" is used for daytime values. As illustrated in Fig. 4, the daytime values of VSH/H_p have a strong negative tendency with the velocity term of Eq. (1), while this correlation becomes much poorer during the nighttime. We speculate that this scatter is likely due to the day-to-day and local time variabilities in the thermospheric neutral winds and electric fields. Direct observational studies are needed to verify whether or not the relationship between VSH and H_p is sensitive to the dynamics in the ionosphere, as predicted in Eq. (1).

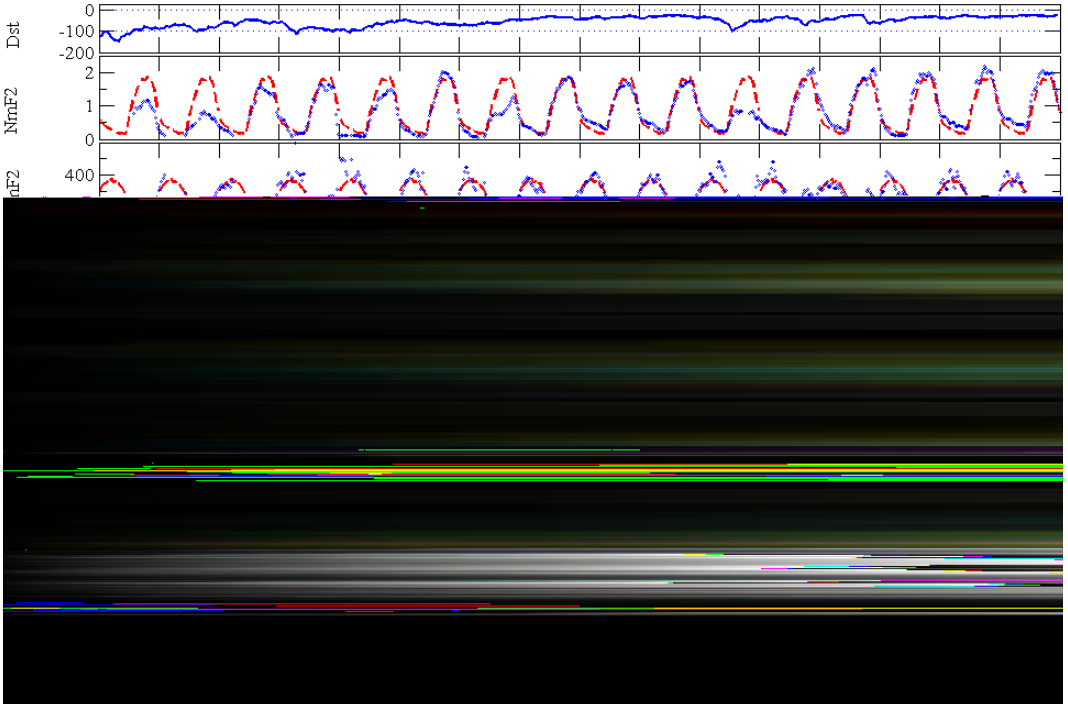

Fig. 5. Geomagnetic index D_{st} and $N_m\mathrm{F}_2$, $h_m\mathrm{F}_2$, VSH, H_p, VSH/H_p, V_o, and (dT_p/dh)/T_p derived from the Millstone Hill ISR experiment during 4 October to 20 October 2002. The dashed curves show the median values, and points for half-hourly averaged values. Here V_o represents values around 500 km in units of m/s, $N_m\mathrm{F}_2$ is in units of 10^{12} m^{-3}, and $h_m\mathrm{F}_2$, VSH and H_p in km.

3.4 The geomagnetic activity effects

The geomagnetic activity effects on the ionosphere are well-known to be complicated and stochastic (e.g. Buonsanto, 1999; Kutiev et al., 2005; Liu et al., 2004; Mendillo, 2006). Although there are poor correlations between geomagnetic indices and ionospheric scale heights (Kutiev et al., 2006; Liu et al., 2007; Stankov and Jakowski, 2006b), enhanced geomagnetic activities will increase the variability of the ionospheric scale heights; that is, ionospheric scale heights may greatly deviate from the average pattern under individual disturbed situations, such as the ionogram-derived H_m over Wuhan (Liu et al., 2006), ISR profiles derived VSH and H_m over Arecibo (Liu et al., 2007), and topside scale height inversed from GPS-TEC (Gulyaeva, 2004).

To illustrate the behavior of the ionosphere over Millstone Hill under geomagnetically quiet and disturbed conditions, Fig. 5 plots the variations of ionospheric parameters during 4 October to 20 October 2002 and Fig. 6 for 21 October to 5 November 2002. Panels in Figs. 5 and 6, from the top to the bottom, are for geomagnetic index D_{st} and $N_m\mathrm{F}_2$, $h_m\mathrm{F}_2$, VSH, H_p, VSH/H_p, V_o and (dT_p/dh)/T_p, respectively. The dashed lines denote values serving as the reference level and circle symbols ("o") for half-hourly averaged values.

As seen from Fig. 5, there are appreciable differences in ionospheric parameters under geomagnetically quiet and disturbed conditions. Generally ionospheric parameters follow their median behavior under geomagnetically quiet conditions. Typical examples can be found on day 286 and day 293. During the first active interval, $N_m\mathrm{F}_2$ is markedly depressed below its reference level on days 277–279 and on day 281. Apart from a significant evening lift on day 281, $h_m\mathrm{F}_2$ presented no significant deviation from the reference level. In contrast, the magnitude of VSH and H_p deviated remarkably from the reference level, with enhancements on days 277 and 278. Enhanced variability was presented in VSH/H_p on day 278 and in the early hours of day 279, in V_o near the morning peak on day 278. It is interesting that on day 281, all parameters strongly deviate from their reference levels: $N_m\mathrm{F}_2$, V_o and (dT_p/dh)/T_p were depressed, while $h_m\mathrm{F}_2$, VSH, H_p and VSH/H_p were greatly enhanced.

During the daytime of day 283, when the geomagnetic activity is moderate and tends to recover to its normal state, there is a remarkable depletion in $N_m\mathrm{F}_2$, which can be explained with the storm-time induced changes of neutral compositions and temperature. Accompanying the $N_m\mathrm{F}_2$ depletion, a huge enhancement occurred in $h_m\mathrm{F}_2$, VSH and H_p. However, during the daytime huge $N_m\mathrm{F}_2$ depletion, no marked change is presented in $h_m\mathrm{F}_2$.

During the second active interval, depletions were presented in V_o and (dT_p/dh)/T_p. Although $N_m\mathrm{F}_2$, $h_m\mathrm{F}_2$ and H_p quickly recovered to their normal states, great deviations were still present in VSH, VSH/H_p, V_o and (dT_p/dh)/T_p for a further 2–3 days.

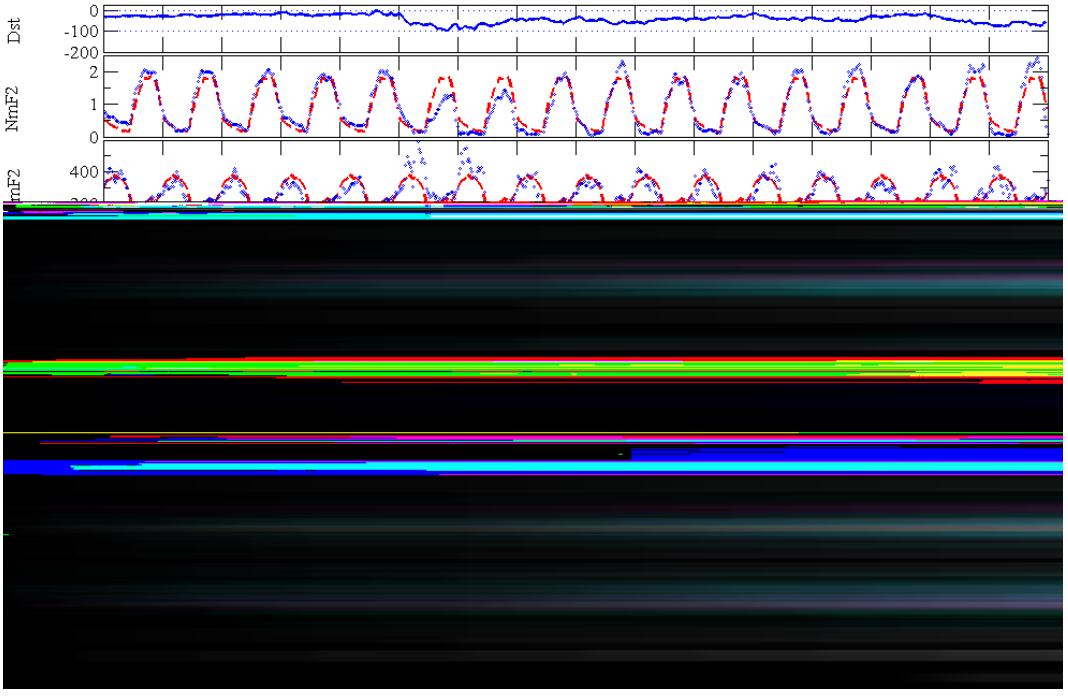

Fig. 6. Same as Fig. 5, but for 21 October to 5 November 2002.

As seen from Fig. 6, during the third active interval, $N_m\mathrm{F}_2$ and $(\mathrm{d}T_p/\mathrm{dh})/T_p$ decreased while $h_m\mathrm{F}_2$, H_p and VSH increased remarkably on days 297–298. In contrast, another type of effect is found on days 306–307; that is, there is the classic pattern of a dusk effect (e.g. Buonsanto, 1999) in $N_m\mathrm{F}_2$, namely a large enhancement seen in $N_m\mathrm{F}_2$ during the afternoon and evening hours followed by a negative phase. The dusk effect is believed to be caused by the magnetospheric convection electric fields (e.g. Mendillo, 2006). Accompanying the negative phase in $N_m\mathrm{F}_2$ on day 307, VSH and H_p were enlarged, and VSH/H_p obviously deviated from the reference level due to the enhanced variability of VSH/H_p.

As has been mentioned by Liu et al. (2007), VSH can provide information on the shape of topside electron density profiles. The ionosphere follows the median behavior under geomagnetic quiet conditions. As a result, ionospheric parameters, such as $N_m\mathrm{F}_2$, $h_m\mathrm{F}_2$, VSH and H_p, generally follow their median diurnal variations. In contrast, the ionosphere is modified under disturbed conditions. We have noted that a negative phase and dusk effect in $N_m\mathrm{F}_2$ are present during this experiment. In the presented case, large differences are detected in VSH and H_p under quiet and disturbed magnetic conditions. The variability of the scale heights becomes enhanced under disturbed conditions, indicating that the shape of the topside electron density profiles are appreciably changed due to the storm impacts.

4 Summary

Data of $N_m\mathrm{F}_2$, $h_m\mathrm{F}_2$, VSH,V_o and $(\mathrm{d}T_p/\mathrm{dh})/T_p$ andH_p deduced from the ISR measurement (4 October to 4 November 2002) at Millstone Hill are analyzed to explore the variations of the ionosphere. The main results are summarized as follows:

1. This statistical analysis identifies a clear average pattern of ionospheric scale heights VSH, H_m, and H_p over Millstone Hill; that is, the diurnal behaviors of the median VSH and H_m are found to be greatly similar to each other and are not so tightly correlated with the plasma scale height H_p or the plasma temperature.

2. In combining this investigation with that of Luan et al. (2006), evidence exists that both contributions from the temperature structure and diffusion processes can greatly control the shape of the electron density profile and the ratio VSH/H_p in the topside ionosphere over Millstone Hill. Following the theoretical prediction, the values of VSH/H_p tend to decrease as $(\mathrm{d}T_p/\mathrm{dh})/T_p$ becomes larger. This feature is also detected at a low-latitude station Arecibo (Liu et al., 2007). A similar correlation seems to exist between VSH/H_p and the dynamical processes, while further measurements are still required.

3. Large differences are detected in VSH and H_p, as well as in $N_m\mathrm{F}_2$, $h_m\mathrm{F}_2$, and $(\mathrm{d}T_p/\mathrm{dh})/T_p$ under geomagnetic

quiet and disturbed conditions. Generally ionospheric parameters follow their median behaviors under geomagnetically quiet conditions, while the variability of the scale heights and other parameters is enhanced under disturbed conditions. In the present case, both VSH and H_p increased significantly during storm times, indicating that the geomagnetic activity has a major impact on the behavior of ionospheric scale heights. However, to understand the complexity of the perturbations, more studies are deserved.

Acknowledgements. This study made use of the Millstone Hill ISR data. The Millstone Hill incoherent scatter radar is supported by a cooperative agreement between the National Science Foundation of USA and the Massachusetts Institute of Technology. WDC-C2 provides the geomagnetic indices D_{st}, A_p and AE data. This research was supported by National Natural Science Foundation of China (40725014, 40574071), and National Important Basic Research Project (2006CB806306).

Topical Editor M. Pinnock thanks I. Kutiev and another anonymous referee for their help in evaluating this paper.

References

Belehaki, A., Marinov, P., Kutiev, I., Jakowski, N., and Stankov, S.: Comparison of the topside ionosphere scale height determined by topside sounders model and bottomside digisonde profiles, Adv. Space Res., 37, 963–966, 2006.

Bilitza, D.: International reference ionosphere 2000, Radio Sci., 36(2), 261–275, 2001.

Bilitza, D., Reinisch, B. W., Radicella, S. M., Pulinets, S., Gulyaeva, T., and Triskova, L.: Improvements of the International reference ionosphere model for the topside electron density profile, Radio Sci., 41, RS5S15, doi:10.1029/2005RS003370, 2006.

Buonsanto, M. J.: Ionospheric storms- A review, Space Sci. Rev., 88, 563–601, 1999.

Gulyaeva, T. L.: Incorporation of topside half peak density anchor point in IRI, Adv. Space Res., 34, 1993–1997, 2004.

Huang, X. and Reinisch, B. W.: Vertical electron profiles from the Digisonde network, Adv. Space Res., 18(6), 121–129, 1996.

Huang, X. and Reinisch, B. W.: Vertical electron content from ionograms in real time, Radio Sci., 36(2), 335–342, 2001.

Isham, B., Tepley, C. A., Sulzer, M. P., Zhou, Q. H., Kelley, M. C., Friedman, J. S., and González, S. A.: Upper atmospheric observations at the Arecibo Observatory: Examples obtained using new capabilities, J. Geophys. Res., 105(A8), 18 609–18 637, 2000.

Kutiev, I., Watanabe, S., Otsuka, Y., and Saito, A.: Total electron content behavior over Japan during geomagnetic storms, J. Geophys. Res., 110(A1), A01308, doi:10.1029/2004JA010586, 2005.

Kutiev, I. and Marinov, P.: Topside sounder model of scale height and transition height characteristics of the ionosphere, Adv. Space Res., 39(5), 759–766, 2007.

Kutiev, I. S., Marinov, P. G., and Watanabe, S.: Model of topside ionosphere scale height based on topside sounder data, Adv. Space Res., 37, 943–950, 2006.

Lei, J., Liu, L., Wan, W., and Zhang, S.-R.: Variations of electron density based on long-term incoherent scatter radar and ionosonde measurements over Millstone Hill, Radio Sci., 40, RS2008, doi:10.1029/2004RS003106, 2005.

Lei, J., Liu, L., Wan, W., Zhang, S.-R., and van Eyken, A. P.: Comparison of the first long-duration IS experiment measurements over Millstone Hill and EISCAT Svalbard radar with IRI2001, Adv. Space Res., 37, 1102–1107, 2006.

Liu L., Wan, W., Lee, C. C., Ning, B., and Liu, J. Y.: The low latitude ionospheric effects of the April 2000 magnetic storm near the longitude 120° E, Earth Planets Space, 56, 607–612, 2004.

Liu, L., Wan, W., and Ning, B.: A study of the ionogram derived effective scale height around the ionospheric *hm*F2, Ann. Geophys., 24, 851–860, 2006, http://www.ann-geophys.net/24/851/2006/.

Liu, L., Le, H., Wan, W., Sulzer, M. P., Lei, J., and Zhang, M.-L.: An analysis of the scale heights in the lower topside ionosphere based on the Arecibo incoherent scatter radar measurements, J. Geophys. Res., 112, A06307, doi:10.1029/2007JA012250, 2007.

Luan, X., Liu, L., Wan, W., Lei, J., Zhang, S.-R., Holt, J. M., and Sulzer, M. P.: A study of the shape of the topside electron density profile derived from incoherent scatter radar measurements over Arecibo and Millstone Hill, Radio Sci., 41, RS4006, doi:10.1029/2005RS003367, 2006.

Mendillo, M.: Storms in the ionosphere: patterns and processes for total electron content, Rev. Geophys., 44, RG4001, doi:10.1029/2005RG000193, 2006.

Oyama, K.-I., Watanabe, S., Su, Y., Takahashi, T., and Hiro, K.: Seasonal, local time, and longitudinal variations of electron temperature at the height of ∼600 km in the low latitude region, Adv. Space Res., 18(6), 269–278, 1996.

Reinisch, B. W. and Huang, X.: Deducing topside profiles and total electron content from bottomside ionograms, Adv. Space Res., 27(1), 23–30, 2004.

Reinisch, B. W., Huang, X., Belehaki, A., Shi, J., Zhang, M., and Ilma, R.: Modeling the IRI topside profile using scale height from ground-based ionosonde measurements, Adv. Space Res., 34, 2026–2031, 2004.

Rishbeth, H. and Garriott, O. K.: Introduction to ionospheric physics, 331 pp., Academic Press, New York, 1969.

Sharma, D. K., Rai, J., Israil, M., and Subrahmanyam, P.: Diurnal, seasonal and longitudinal variations of ionospheric temperatures of the topside F region over the Indian region during solar minimum (1995–1996), J. Atmos. Solar-Terr. Phys., 67, 269–274, 2005.

Stankov, S. M. and Jakowski, N.: Topside plasma scale height retrieved from radio occultation measurements, Adv. Space Res., 37, 958–962, 2006a.

Stankov, S. M. and Jakowski, N.: Topside ionospheric scale height analysis and modeling based on radio occultation measurements, J. Atmos. Solar-Terr. Phys., 68, 134–162, 2006b.

Stankov, S. M., Jakowski, N., Heise, S., Muhtarov, P., Kutiev, I., and Warnant, R.: A new method for reconstruction of the vertical electron density distribution in the upper ionosphere and plasmasphere, J. Geophys. Res., 108(A5), 1164, doi:10.1029/2002JA009570, 2003.

Tepley, C. A.: Current developments at Arecibo for research in the atmospheric sciences at low latitudes, J. Atmos. Solar-Terr. Phys., 59(13), 1679–1686, 1997.

Zhang, M.-L., Reinisch, B. W., Shi, J. S., Wu, S., and Wang, X.: Diurnal and seasonal variation of the ionogram-derived scale height at the F2 peak, Adv. Space Res., 37, 967–971, 2006.

Zhang, S.-R., Holt, J. M., Zalucha, A. M., and Amory-Mazaudier, C.: Midlatitude ionospheric plasma temperature climatology and empirical model based on Saint Santin incoherent scatter radar data from 1966 to 1987, J. Geophys. Res., 109, A11311, doi:10.1029/2004JA010709, 2004.

Zhang, S.-R., Holt, J. M., Erickson, P. J., Lind, F. D., Foster, J. C., van Eyken, A. P., Zhang, Y., Paxton, L. J., Rideout, W. C., Goncharenko, L. P., and Campbell, G. R.: October 2002 30-day incoherent scatter radar experiments at Millstone Hill and Svalbard and simultaneous GUVI/TIMED observations, Geophys. Res. Lett., 32, L01108, doi:10.1029/2004GL020732, 2005.